Journal of Sound and Vibration (1998) **212**(2), 311–319

MELNIKOV'S METHOD FOR NON-LINEAR OSCILLATORS WITH NON-LINEAR EXCITATIONS

J. GARCIA-MARGALLO AND J. D. BEJARANO

Departamento de Física, Facultad de Ciencias, Universidad de Extremadura, 06071 Badajoz, Spain

(*Received* 22 *July* 1997, *and in final form* 25 *November* 1997)

The response of a non-linear oscillator of the form $\ddot{x} + f(A, B, x) = \varepsilon g(E, \mu, w, k, t)$, where $f(A, B, x)$ is an odd non-linearity and ε is small, for $A < 0$ and $B > 0$ is considered. The homoclinic orbits for the unperturbed system are obtained by using Jacobian elliptic functions with the generalized harmonic balance method. Also the chaotic limits of this equation are studied with a generalized Melnikov function, $M^0(E, \mu, \dot{x}, w, k, t_0)$, depending on the variable k. A function $R^0(E, \mu, w, k)$ is defined such that there only exists chaotic motion if $E/\mu > R^0$ with k from 0·51 to 0·99. It is demonstrated with Poincaré maps in the phase plane that there is good agreement between these predictions and the numerical simulations of the Duffing–Holmes oscillator using the fourth-order Runge–Kutta method of numerical integration.

1. INTRODUCTION

Numerous qualitative analyses have demonstrated the existence and characteristics of chaotic motions in deterministic non-linear systems. It is interesting to know the parameter values below which no periodic motions would occur in the forced non-linear oscillator. One of the models which has been most extensively studied is the Duffing equation.

Kapitaniak [1] described a method, based on harmonic balance, for controlling chaotic behaviour of the Duffing equation

$$\ddot{x} + a\dot{x} + bx + cx^3 = B_0 + B_1 \cos \Omega t,$$

for $a = 0{\cdot}05$, $b = 0{\cdot}00$, $c = 1{\cdot}00$, $B_0 = 0{\cdot}03$, $B_1 = 0{\cdot}16$ and $\Omega = 0{\cdot}97$, showing that chaotic behaviour results via a period-doubling bifurcation.

Xu and Cheung [2] use an averaging method and generalized harmonic functions to study the approximate solutions to the Duffing oscillator with a periodic external force

$$\ddot{x} + m_1 x + m_2 x^3 = \varepsilon(-\mu x + E \cos \Omega t).$$

For $m_1 = 2{\cdot}0$, $m_2 = 4{\cdot}0$, $\varepsilon = 0{\cdot}1$, $\mu = 0{\cdot}2$ and $E = 2{\cdot}0$ there are one or three limit cycles for $0{\cdot}0 \leqslant \Omega \leqslant 4{\cdot}5$.

Awrejcewicz and Mrozowski [3] present the chaotic dynamics of a particular van der Pol non-linear oscillator having Duffing-type stiffness

$$\dot{y} = z, \qquad \dot{z} = \varepsilon(1 - y^2)\dot{y} - \delta y - \gamma y^3 - \alpha \operatorname{sgn} \dot{y} + p_0 \nu^2 \cos \nu t.$$

They utilize an averaging technique to obtain information regarding the bifurcation behaviour of the vibrating system and then analyse numerically the chaotic behaviour of the oscillator for parameters near the bifurcation curves. The authors report that for

0022–460X/98/170311 + 09 \$25.00/0/sv971443

$\varepsilon = 8{\cdot}00$, $p_0 = 1{\cdot}00$, $\delta = -28{\cdot}00$, $\gamma = 37{\cdot}33$, $\alpha = 21{\cdot}99$, $\omega = -8{\cdot}00$, and $\nu = 14{\cdot}00$ this equation has chaotic behaviour.

Pezeshki *et al*. [4] have studied the Duffing equation as it undergoes a period-doubling sequence to chaos using polyspectral techniques.

Show and Wiggins [5] use a variation of Melnikov's method developed for a slowly varying oscillator. When the system is perturbed by external excitations and dissipative forces, the homoclinic motions can break into homoclinic tangles providing the conditions for chaotic motions. The validity of the Melnikov method is checked in the Duffing equation, with excellent results.

Some examples of physical systems in which chaos has been found, have been described in the work of Van Dooren [6], Szemplinska-Stupnicka [7], Tongue [8, 9], Ueda [10], Holmes and Rand [11], Hockett and Holmes [12], and Moon [13].

Moon and Li [14] observe a fractal-looking basin boundary for forced periodic motions of a particle in a Duffing potential in a numerical simulation. The fractal structure seems to be correlated with the appearance of homclinic orbits in the Poincaré map as calculated by Holmes [15], using the method of Melnikov [16].

Guckenheimer and Holmes [17] develop a theoretical study of the equation $\dot{x} = f(x) + \varepsilon g(x, t)$ using the method of Melnikov to derive a necessary criterion for chaotic motion based on the existence of transverse homoclinic orbits in the Poincaré map. This criterion gives the condition for the intersection of stable and unstable manifolds associated with the saddle point of the Poincaré map.

In this work the Duffing-Holmes oscillator central to the analysis of chaos in simple mechanical systems is studied, that is

$$\ddot{x} + Ax + Bx^3 = \varepsilon(-\mu x + E\cos\phi_3),$$

for $A < 0$, $B > 0$, where $\phi_3 = \mathrm{am}\,(\omega t; k^2)$ [18] is the amplitude of the incomplete elliptical integral of the first kind, and k^2 is the modulus of Jacobian elliptic functions.

In this treatment in terms of elliptic functions, ϕ_3 will be the argument of $\sin\phi_3$ and $\cos\phi_3$ so that $\sin\phi_3 = \sin\,(\omega t; k^2) = \sin u$, $\cos\phi_3 = \mathrm{cn}\,(\omega t; k^2) = \mathrm{cn}\,u$; i.e., $\phi_3 \equiv \int \mathrm{d}n\,u\,\mathrm{d}u$.

The homoclinic orbits for the unperturbed system, $\varepsilon = 0$, are obtained by using Jacobian elliptic functions with the generalized harmonic balance method. To analyse the chaos of this equation the Holmes–Melnikov method is used. This analytical method detects transverse homoclinic points in differential equations corresponding to small perturbations of integrable systems. If the Melnikov function has simple zeros, then, for sufficiently small ε, chaotic motion exist near the separatrix. In consequence only necessary conditions for chaos are obtained from this type of analysis, and therefore always sufficient conditions for the suppression of chaos. The method is in consequence fundamental for predicting the inhibition of chaos.

To check the theoretical results of the Holmes–Melnikov method a fourth order Runge–Kutta numerical integration is used to obtain the Poinaré maps.

2. THE METHODS

A method is developed which enables one to study the Poincaré map for time-periodic systems of the form

$$\dot{x} = u,$$
$$\dot{u} = f(A, B, x) + \varepsilon g(E, \mu, u, w, k^2, t), \tag{1}$$

where the unperturbed system, $\varepsilon = 0$, is an integrable Hamiltonian system, and $\varepsilon g(E, \mu, u, w, k^2, t)$ is a small perturbation which need not itself be Hamiltonian.

The basic idea to be introduced here, due to Melnikov [16], is to make use of the globally computable solutions of the unperturbed integrable system in the computation of perturbed solutions. To do this one must first ensure that the perturbation calculations are uniformly valid on arbitrarily long or semi-infinite time intervals.

For simplicity, assume that the unperturbed system, $\varepsilon = 0$, is an integrable Hamiltonian system with $f_1 = \partial \mathscr{H}/\partial u$, $f_2 = -\partial \mathscr{H}/\partial x$, with a fixed hyperbolic saddle point x_0 and possesses a homoclinic orbit or separatrix $x_s(t)$ such that

$$\lim_{t\to\infty} x_s(t) = x_0.$$

It is supposed that, in equation (1), the perturbative term g introduces dissipation and a non-autonomous forcing of period T.

The perturbed phase space must be extended to three dimensions (E, μ, k^2, t) and the motion can be studied from the Poinaré map for $t = \text{const} \pmod{T}$.

The perturbed stable and unstable manifolds can be identified on the Poincaré map, but now in general their evolution is different and with sufficient damping the manifolds never intersect. Nevertheless if the ratio between damping and forcing is sufficiently small, the stable and unstable manifolds intersect transversely.

The assumption $\varepsilon = 0$ immediately implies that the unperturbed Poincaré map has a hyperbolic saddle point x_0 and that the closed curve representing the separatrix is filled with non-transverse homoclinic points for this Poincaré map. This highly degenerate structure is expected to break under the perturbation $\varepsilon g(E, \mu, u, w, k^2, t)$, and perhaps to yield transverse homoclinic orbits or no homoclinic points at all. The goal of this section is the development of a method to determine what happens in specific cases. In particular, this method will enable one to prove the existence of transverse homoclinic points and homoclinic bifurcations, and is a signal for chaotic behaviour that is local in the sense that it occurs for trajectories with initial conditions near the non-perturbed separatrix.

To test for transverse homoclinic intersections, use is made of the well-known Melnikov function [16, 17], which is a measure of the distance between the perturbed stable and unstable manifolds in the Poincaré map. Define the Melnikov function as

$$M(t_0) = \int_{-\infty}^{\infty} f[q^0(t - t_0)] * g[q^0(t - t_0), t]\, \mathrm{d}t, \tag{2}$$

where $q^0(t - t_0)$ are the starting orbits for finite times. If $M(t_0)$ has simple zeros and is independent of ε, then, for $\varepsilon > 0$ sufficiently small the manifolds intersect transversely.

3. STUDY OF THE OSCILLATOR

Equation (1) can be written in the form

$$\begin{aligned} \dot{x} &= u, \\ \dot{u} &= -Ax - Bx^3 + \varepsilon(-\mu u + E \cos \phi_3), \end{aligned} \tag{3}$$

for $A < 0$ and $B > 0$, where $\phi_3 = \text{am}\,(wt; k^2)$ [18], and $k^2 = m$ the parameter of the Jacobian function. The force amplitude E and the damping μ are variable parameters, and ε is a small parameter. The unperturbed system $\varepsilon = 0$, is Hamiltonian with a total energy

$$\mathscr{H} = T + U = 1/2u^2 + 1/2Ax^2 + 1/4Bx^4,$$

has centres at $(x, u) = (\pm\sqrt{-A/B}, 0)$ and a hyperbolic saddle point at $(0, 0)$. The separatrix consists of two homoclinic orbits Γ^0_+, Γ^0_- and the point $x_0 = (0, 0)$.

The unperturbed system is

$$\ddot{x} + Ax + Bx^3 = 0, \tag{4}$$

and following references [19, 20], the solutions corresponding to this equation are

$$x = a\cos\phi_3 = a\,\mathrm{cn}\,(\Omega t; m). \tag{5}$$

Differentiating equation (5) twice, and substituting into equation (4) gives

$$a\{[A + \Omega^2(2m-1)]\,\mathrm{cn} + [Ba^2 - 2m\Omega^2]\,\mathrm{cn}^3\} = 0. \tag{6}$$

Using the method of harmonic balance [21, 22], a generalized Fourier expansion, if the expansion is limited to the first harmonic, gives

$$a\{[A + \Omega^2(2m-1)] + (3/4)[Ba^2 - 2m\Omega^2]\}\cos\phi_3 = 0. \tag{7}$$

Setting the coefficient of $\cos\phi_3$ to zero gives

$$A + \Omega^2(2m-1) = 0 \qquad \text{and} \qquad Ba^2 - 2m\Omega^2 = 0. \tag{8}$$

From equation (8)

$$\Omega = [A/(1-2m)]^{1/2} \qquad \text{and} \qquad B = \frac{2m\Omega^2}{a^2}, \tag{9}$$

and from these two equations

$$a = [2mA/B(1-2m)]^{1/2}. \tag{10}$$

Therefore the generalized orbits are

$$(x, u) = \{\sqrt{2mA/B(1-2m)}\,\mathrm{cn}\,[\sqrt{A/(1-2m)}t; m],$$
$$-\frac{A}{(1-2m)}\sqrt{2m/B}\,\mathrm{sn}\,[\sqrt{A/(1-2m)}t; m]\,\mathrm{dn}\,[\sqrt{A/(1-2m)}t; m]\}. \tag{11}$$

For $m = 1$, one has the homoclinic orbits, and $\mathrm{cn}\,u = \mathrm{sech}\,u$, $\mathrm{sn}\,u = \tanh u$ and $\mathrm{dn}\,u = \mathrm{sech}\,u$, so that equation (11) becomes

$$\Gamma^0_\pm = \{\pm\sqrt{-2A/B}\,\mathrm{sech}\,[\sqrt{-A}t],\ \mp\sqrt{2A^2/B}\tanh[\sqrt{-A}t]\,\mathrm{sech}\,[\sqrt{-A}t]\}. \tag{12}$$

If the perturbation g is defined from a time-dependent Hamiltonian function $G(x, u)$ with $g_1 = \partial G/\partial u$, $g_2 = -\partial G/\partial x$, then the generalized Melnikov function for the homoclinic orbit Γ^0_+ is

$$M^+(t_0) = \int_{-\infty}^{\infty} f[\Gamma^0_+(t)] * \mathbf{g}[\Gamma^0_+(t), t + t_0]\,\mathrm{d}t, \tag{13}$$

with an analogous definition for Γ^0_-. Here the wedge product is defined by $\mathbf{f} * \mathbf{g} = f_1 g_2 - f_2 g_1$. In the present case,

$$f_1 = u, \qquad g_1 = 0.$$
$$f_2 = -Ax - Bx^3, \qquad g_2 = E\cos\phi_3 - \mu u,$$

so that $\mathbf{f} * \mathbf{g} = u(E\cos\phi_3 - \mu u)$ and

$$M^+(t_0) = \int_{-\infty}^{\infty} u^0(t)[E\cos\phi_3(t+t_0) - \mu u^0(t)]\,\mathrm{d}t$$

$$= -\left[\frac{2A^2}{B}\right]^{1/2} E\int_{-\infty}^{\infty} \tanh[\sqrt{-A}t]\,\mathrm{sech}[\sqrt{-A}t]\cos\phi_3(t+t_0)\,\mathrm{d}t$$

$$-\left[\frac{2A^2}{B}\right]\mu\int_{-\infty}^{\infty} \tanh^2[\sqrt{-A}t]\,\mathrm{sech}^2[\sqrt{-A}t]\,\mathrm{d}t. \quad (14)$$

Therefore if the Jacobian elliptic function, cn, is expanded in a Fourier series [23], then

$$\cos\phi_3(t+t_0) = \mathrm{cn}[w(t+t_0); k^2] = \frac{2\pi}{kK}\sum_{n=0}^{\infty}\frac{q^{n+1/2}}{1+q^{2n+1}}\cosh\left[(2n+1)\frac{\pi w(t+t_0)}{2K}\right]$$

$$= \frac{2\pi}{kK}\sum_{n=0}^{\infty} 1/2\,\mathrm{sech}\left[(2n+1)\frac{\pi K'}{2K}\right]\left\{\cosh(2n+1)\frac{\pi wt}{2K}\cos(2n+1)\frac{\pi wt_0}{2K}\right.$$

$$\left. -\sin(2n+1)\frac{\pi wt}{2K}\sin(2n+1)\frac{\pi wt_0}{2K}\right\}. \quad (15)$$

Here $K = K(k)$ is the complete elliptic integral of the first kind, $K' = K'(k) = K(k')$ the associated complete elliptic integrals of the first kind, where k' is termed the complementary modulus and is related to k by $k' = \sqrt{1-k^2}$, and $k = m^{1/2}$.

Then substituting expression (15) into (14) one has:

$$M^+(t_0) = -\frac{4A^2\mu}{3B\sqrt{-A}} + \left[\frac{2A^2}{B}\right]^{1/2} E * \frac{\pi^3 w}{2kK^2(-A)}\left[\sum_{n=0}^{\infty}(2n+1)\,\mathrm{sech}\left[(2n+1)\frac{\pi K'}{2K}\right] *\right.$$

$$\left.\mathrm{sech}\left[(2n+1)\frac{\pi^2 w}{4K\sqrt{-A}}\right]\sin\left[(2n+1)\frac{\pi wt_0}{2K}\right]\right]. \quad (16)$$

This Melnikov function has a quadratic zero with respect to t_0:

$$\left.\frac{\partial M^+(t_0)}{\partial t_0}\right|_{t_0=\tau} = \left[\frac{2A^2}{B}\right]^{1/2} E * \frac{\pi^3 w}{2kK^2(-A)}\left[\sum_{n=0}^{\infty}(2n+1)\left[(2n+1)\frac{\pi w}{2K}\right]\right.$$

$$\mathrm{sech}\left[(2n+1)\frac{\pi K'}{2K}\right]\mathrm{sech}\left[(2n+1)\frac{\pi^2 w}{4K\sqrt{-A}}\right]$$

$$\left.\left.\cos\left[(2n+1)\frac{\pi wt_0}{2K}\right]\right]\right|_{t_0=\tau} = 0, \quad (17)$$

so that $\cos[(2n+1)(\pi w\tau)/2K] = 0$, where $(2n+1)(\pi w\tau/2K) = (2n+1)\pi/2$, and $\tau = K/w$. Also,

$$\left.\frac{\partial^2 M^+(t_0)}{\partial t_0^2}\right|_{t_0=\tau} = \left[\frac{2A^2}{B}\right]^{1/2} E * \frac{\pi^3 w}{2kK^2(-A)}\left[\sum_{n=0}^{\infty}(2n+1)\left[(2n+1)\frac{\pi w}{2K}\right]^2\right.$$

$$\left.\operatorname{sech}\left[(2\mathrm{n}+1)\frac{\pi K'}{2K}\right]\operatorname{sech}\left[(2n+1)\frac{\pi^2 w}{4K\sqrt{-A}}\right]\sin\left[(2n+1)\frac{\pi w t_0}{2K}\right]\right]_{t_0=\tau} \neq 0,$$

since

$$\sin\left[(2n+1)\frac{\pi w\tau}{2K}\right] = \sin\left[(2n+1)\frac{\pi w}{2K}\frac{K}{w}\right] = (-1)^n,$$

so that

$$M^+(t_0)|_{t_0=\tau} = -\frac{4A^2\mu}{3B\sqrt{-A}} + \left[\frac{2A^2}{B}\right]^{1/2} E * \frac{\pi^3 w}{2kK^2(-A)}\left[\sum_{n=0}^{\infty}(-1)^n(2n+1)\right.$$

$$\left.\operatorname{sech}\left[(2n+1)\frac{\pi K'}{2K}\right] * \operatorname{sech}\left[(2n+1)\frac{\pi^2 w}{4K\sqrt{-A}}\right]\right] = 0.$$

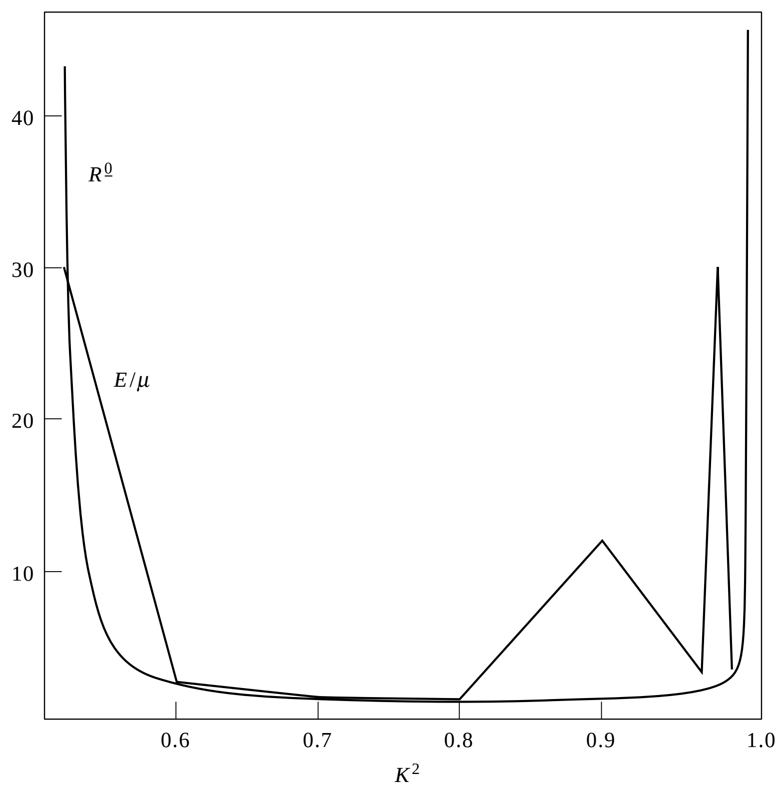

Figure 1. The analytical dependence of R^0 and the numerically calculated dependence of E/μ on k^2.

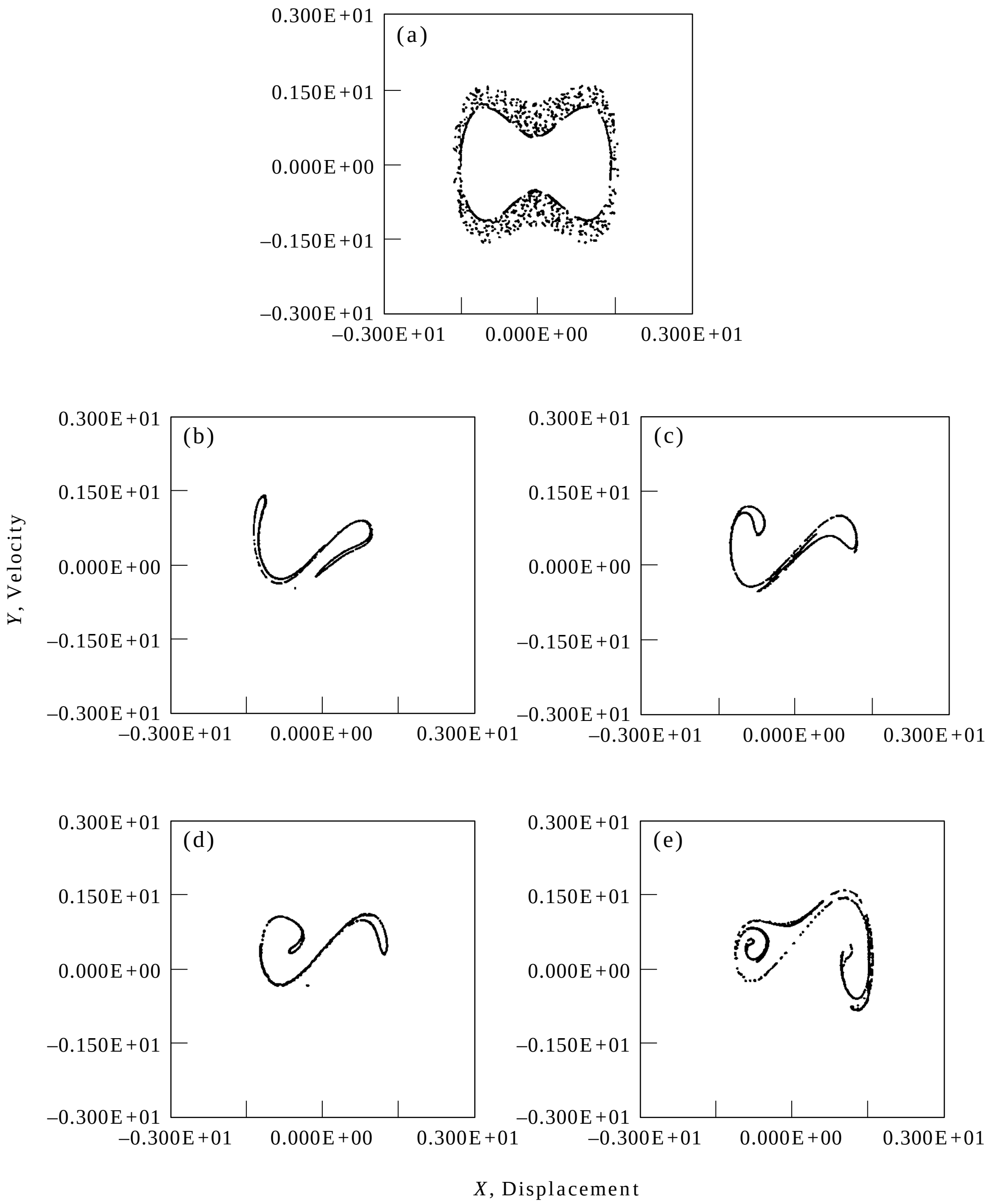

Figure 2. The Poincaré map for: (a) non-chaotic motion for $k^2 = 0{\cdot}51$ and $E/\mu = 2000$, and chaotic motion for (b) $k^2 = 0{\cdot}60$ and $E/\mu = 2{\cdot}860$, (c) $k^2 = 0{\cdot}70$ and $E/\mu = 1{\cdot}666$, (d) $k^2 = 0{\cdot}80$ and $E/\mu = 1{\cdot}663$, (e) $k^2 = 0{\cdot}99$ and $E/\mu = 3{\cdot}700$.

If one defines [17]:

$$R^0(E, \mu, w, k) = [8kK^2\sqrt{-A^3}] *$$

$$\left\{3\sqrt{2B}w\pi^3 \sum_{n=0}^{\infty} (-1)^n(2n+1)\,\mathrm{sech}\left[(2n+1)\frac{\pi K'}{2K}\right]\mathrm{sech}\left[(2n+1)\frac{\pi^2 w}{4K\sqrt{-A}}\right]\right\}^{-1}, \quad (18)$$

then since $M^+(t_0)$ has simple zeros and is independent of ε, if $E/\mu > R^0(E, \mu, w, k)$ and for ε sufficiently small, the stable $x^s(t)$ and unstable $x^u(t)$ trajectories intersect transversely, and if $E/\mu < R^0(E, \mu, w, k)$, $x^s(t) \cap x^u(t) = \phi$. Moreover, since $M^+(t_0)$ has quadratic zeros when $E/\mu = R^0(E, \mu, w, k)$ [16], this implies that there is a bifurcation curve in the E, μ plane for each fixed w, tangent to $E = R^0\mu$ at $E = \mu = 0$, on which quadratic homoclinic tangencies occur.

4. COMPARISON WITH NUMERICAL INTEGRATION

It is instructive to compare these analytically derived results for chaotic motion with a numerical integration of the equations. The fourth-order Runge–Kutta method was used to illustrate the more important results with corresponding Poincaré maps. In obtaining the Poincaré maps, the time up to $2000T$ ($T = 4K(k)/\omega$), equivalent to 20 periods, was discarded as an initial transient.

The results for chaotic motion were computed for all parameters and initial conditions fixed near the homoclinic orbit, except k, since $w = w(k)$.

The chaotic motion of equation (3) was studied for $E/\mu > R^0(E, \mu, w, k)$ and varying k^2 from 0·51 to 0·99. Figure 1 shows the analytical dependence of R^0 on k^2, for fixed values of $A = -2{\cdot}5$ and $B = 2{\cdot}0$, computed precisely, $n = 1000$, using MATHEMATICA (R), where εE and $\varepsilon\mu$ are small, and the numerical calculations of E/μ versus k^2 for chaotic motion.

Figure 2 shows Poincaré maps for various values of k^2 and E/μ. For $k^2 = 0{\cdot}51$ (Figure 2(a)) the motion is non-chaotic even for $E/\mu = 2000$, whereas for k^2 greater than this value one finds chaotic motion at values close to 2.

If one compares the analytical calculations with the numerical integrations, Figure 1, it can be seen that there is good agreement between the two except for $k^2 = 0{\cdot}98$, where Ω and w are equal.

As was stated in the Introduction, $R^0(E, \mu, w, k)$ gives a necessary and sufficient condition threshold for avoiding chaotic motion in the system described by equation (3).

5. CONCLUSION

It has been described how to obtain the Melnikov function of the non-linear perturbed system of the differential equation (3), using Jacobian elliptic functions with their parameter k^2 as a variable. It was shown to have a quadratic zero with respect to t_0 for $\tau = K/w$, and a threshold function $R^0(E, \mu, w, k)$ was defined. These two functions depend on the parameter k^2 of the Jacobian elliptic functions.

The analytical results were compared with numerical integration in Figure 1, and this comparison showed the analytical approximations to be very good, and that chaotic motion exists only if $R^0 \leqslant E/\mu$ for $0{\cdot}51 < k^2 < 0{\cdot}99$.

ACKNOWLEDGMENT

We gratefully acknowledge the DGYCIT, Spain (Project PS90-0101) for financial support.

REFERENCES

1. T. Kapitaniak 1993 *Journal of Sound and Vibration* **163**, 182–187. Analytical method of controlling chaos in Duffing's oscillator.

2. Z. Xu and Y. K. Cheung 1994 *Journal of Sound and Vibration* **174**, 563–576. Averaging method using generalized harmonic functions for strongly non-linear oscillators.
3. J. Awrejcewicz and J. Mrozowski 1989 *Journal of Sound and Vibration* **132**, 89–100. Bifurcations and chaos of a particular van der Pol-Duffing oscillator.
4. C. Pezeshki, S. Elgar and R. C. Krishna 1990 *Journal of Sound and Vibration* **137**, 357–368. Bispectral analysis of possessing chaotic motion.
5. W. Show and S. Wiggins 1988 *Physica D* **31**, 190–211. Chaotic dynamics of a whirling pendulum.
6. R. van Dooren 1988 *Journal of Sound and Vibration* **123**, 327–339. On the transition from regular to chaotic behaviour in the Duffing oscillator.
7. W. Szemplinska-Stupnicka 1987 *Journal of Sound and Vibration* **113**, 155–172. Secondary resonances and approximate models of routes to chaotic motion in non-linear oscillators.
8. B. H. Tongue 1986 *Journal of Sound and Vibration* **110**, 69–78. Existence of chaos in a one-degree of freedom system.
9. B. H. Tongue 1987 *Journal of Applied Mechanics* **109**, 695–699. Characteristics of numerical simulations of chaotic systems.
10. Y. Ueda 1979 *Journal of Statistical Physics* **20**, 181–196. Randomly transitional phenomena in the system governed by Duffing's equation.
11. P. J. Holmes and D. A. Rand 1976 *Journal of Sound and Vibration* **44**, 237–253. The bifurcations of Duffing's equation: an application of catastrophe theory.
12. K. Hockett and P. Holmes 1987 *Proceedings of the IEEE* **75**, 1071–1080. Nonlinear oscillators, iterated maps, symbolic dynamics, and knotted orbits.
13. F. C. Moon 1983 *Physical Review Letters* **53**, 962–964. Fractal boundary for chaos in a two-state mechanical oscillator.
14. F. C. Moon and G. X. Li 1985 *Physical Review Letters* **55**, 1439–1442. Fractal basin boundaries and homoclinic orbits for periodic motion in a two-well potential.
15. P. J. Holmes 1979 *Philosophical Transactions of the Royal Society of London* **1394**, 419–448. A nonlinear oscillator with a strange attractor.
16. V. K. Melnikov 1963 *Transactions Moscow Mathematical Society* **12**, 1–57. On the stability of the center for time periodic perturbations.
17. J. Guckenheimer and P. Holmes 1983 *Nonlinear Oscillations, Dynamical Systems and Bifurcations of Vector Fields*. New York: Springer-Verlag.
18. J. D. Bejarano and A. M. Sanchez 1988 *Journal of Mathematical Physics*, **29**, 1847–1853. Generalized exponential, circular and hyperbolic functions for non-linear quantum mechanics.
19. J. G[A]-Margallo and J. D. Bejarano 1987 *Journal of Sound and Vibration* **116**, 591–595. A generalization of the method of harmonic balance.
20. J. G[A]-Margallo, J. D. Bejarano and S. Bravo 1988 *Journal of Sound and Vibration* **125**, 13–21. Generalized Fourier series for the study of limit cycles.
21. R. E. Mickens 1987 *Journal of Sound and Vibration* **111**, 515–518. A generalization of the method of harmonic balance.
22. J. G[A]-Margallo and J. D. Bejarano 1990 *Journal of Sound and Vibration* **136**, 453–466. Generalized Fourier series and limit cycles of generalized van der Pol oscillators.
23. P. D. Byrd and M. D. Friedman 1971 *Handbook of Elliptic Integrals for Engineers and Scientists*. Berlin: Springer-Verlag.
24. I. S. Gradshteyn and I. M. Ryzhik 1981 *Table of Integrals, Series and Products*. New York: Academic Press.